Electronic Supplementary Material (ESI) for Soft Matter.

Supplementary Information

Flexible hydrogels connecting adhesion and wetting

A-Reum Kim[a,1], Surjyasish Mitra[a,2], Sudip Shyam[2], Boxin Zhao[1*] and Sushanta K. Mitra[2*]

[1] Department of Chemical Engineering, Waterloo Institute for Nanotechnology, University of Waterloo, Waterloo, Ontario, N2L 3G1, Canada.
[2] Department of Mechanical & Mechatronics Engineering, Waterloo Institute for Nanotechnology, University of Waterloo, Waterloo, Ontario, N2L 3G1, Canada.

* To whom correspondence should be addressed. E-mail: zhaob@uwaterloo.ca (Boxin Zhao) and skmitra@uwaterloo.ca (Sushanta K. Mitra).

[a] These authors contributed equally.

Table S1.
Physical properties of Acrylamide (AAm) solvent for different monomer weight percentage.

Monomer weight %	Surface tension, γ (mN/m)	Density, ρ (kg/m^3)
2.5	70.9±0.2	999.7
4.0	69.6±0.1	1001.0
6.3	65.7±0.1	1003.1
6.5	65.6±0.2	1003.3
7.0	65.6±0.1	1003.8
7.5	64.8±0.3	1004.3
10.0	64.2±0.2	1006.8
13.0	61.9±0.1	1009.8
20.0	60.6±0.2	1013.3
30.0	57.3±0.1	1019.4

Table S2.
Comparison of elasto-adhesive parameter between our study and certain existing literature

Literature	Top contacting pair	Bottom contacting pair	$E^* R_0/w$
Rimai *et al.* J. Appl. Phys. (1989)	Polystyrene sphere ($E_1 =$ 100 – 1000 MPa)	Polyurethane rubber ($E_2 =$ 5 MPa)	5 – 205
Rimai *et al.* Langmuir (1994)	Glass sphere	Polyurethane rubber ($E_2 =$ 45 kPa)	5 – 67
Style *et al.* Nat. Commun. (2013)	Glass sphere	Silicone gel ($E_2 =$ 3 – 500 kPa)	0.15 – 88
Jensen *et al.* PNAS (2015)	Glass sphere	Silicone gel ($E_2 =$ 5.6 kPa)	1.5 – 3.2
Chakrabarti *et al.* Langmuir (2018)	Polyacrylamide hydrogel sphere ($E_1 =$ 180 – 2367 kPa)	Bare and silanized silicon wafer	750 – 10^4
Present work	Hydrogel sphere ($E_1 =$ 0.0057 – 106.65 kPa), glass sphere	PDMS ($E_2 =$ 3 – 6855 kPa), glass slides	0.05 – 2×10^5

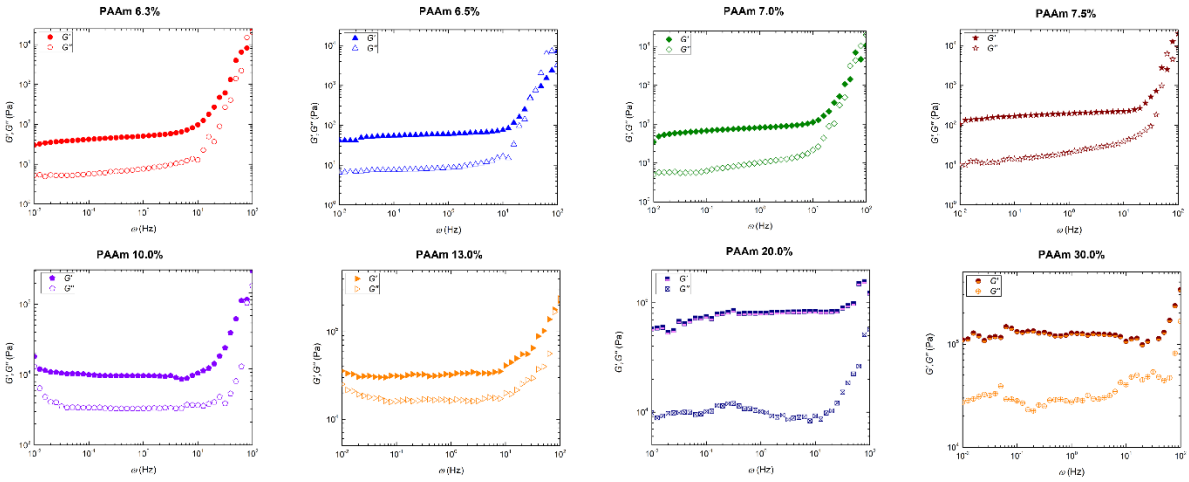

Figure S1. Rheology of hydrogels. Variation of storage modulus (G') and loss modulus (G'') with angular frequency ω for hydrogels with different monomer weight percentages. The static shear modulus G is calculated using $G = \sqrt{G'^2 + G''^2}$ at $\omega = 1$ Hz.

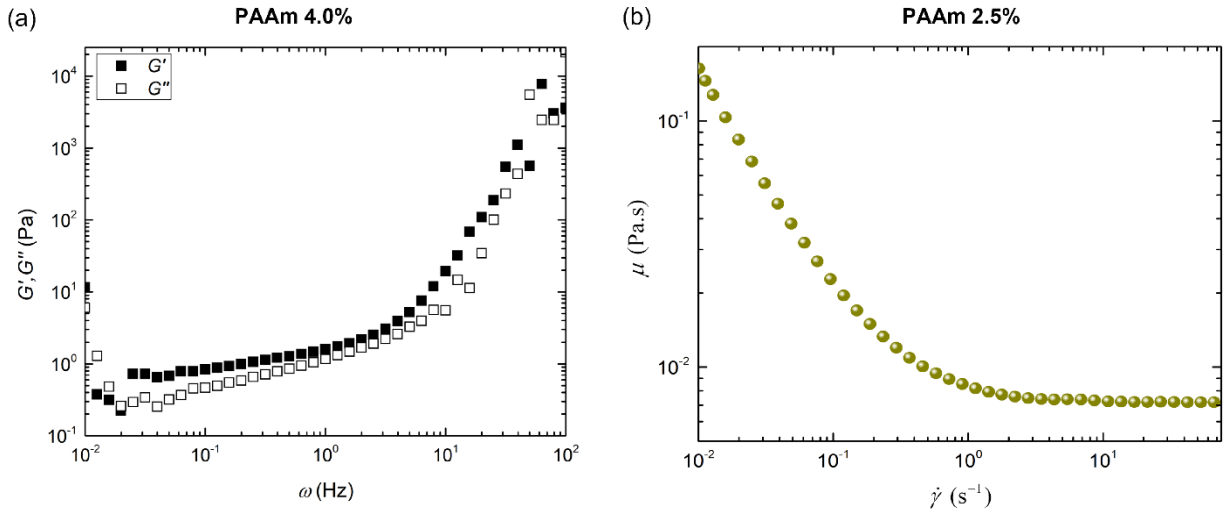

Figure S2. Rheology of hydrogels. (a) Variation of storage modulus (G') and loss modulus (G'') with angular frequency ω for PAAm 13.0%, i.e., hydrogel with 13.0% monomer weight percentage. The static shear modulus G is calculated using $G = \sqrt{G'^2 + G''^2}$ at $\omega = 1$ Hz. (b) Variation of shear viscosity μ with shear rate $\gamma^{\cdot}$ for the liquid hydrogel, i.e., hydrogel with 2.5% monomer weight percentage.

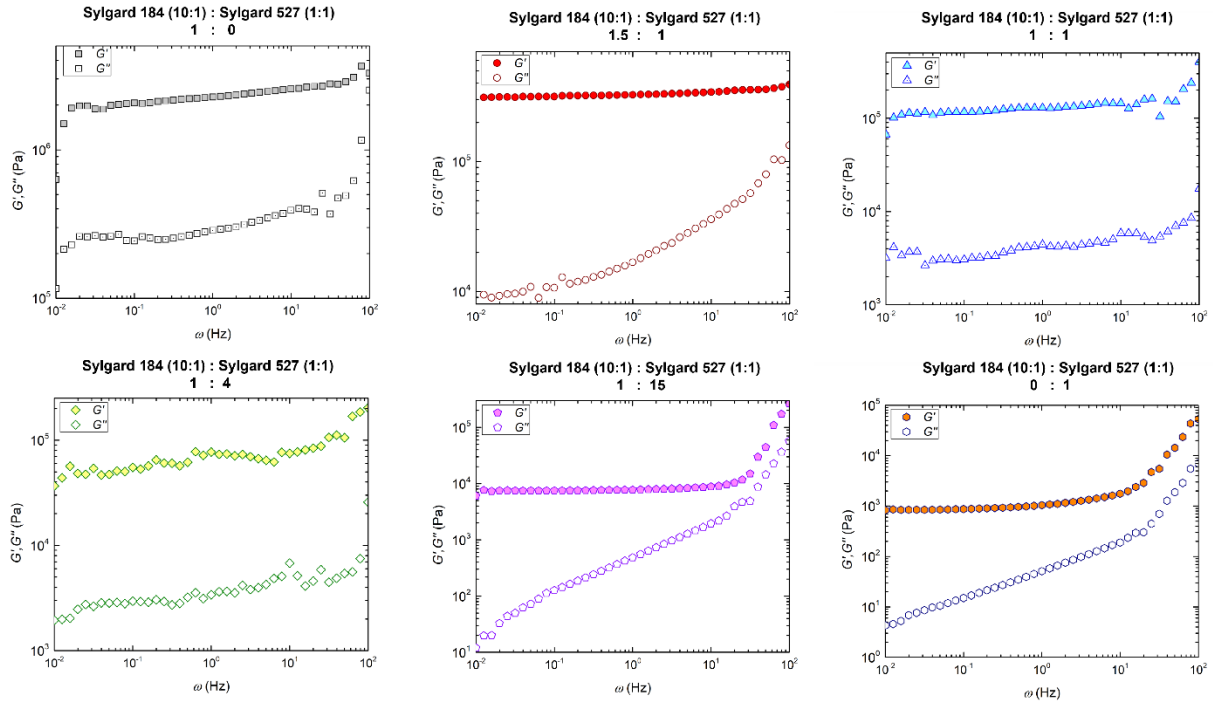

Figure S3. Rheology of soft substrates. Variation of storage modulus (G') and loss modulus (G'') with angular frequency ω for substrates prepared combining Sylgard 184 PDMS (10:1) and Sylgard 527 (1:1) in different weight ratios. The static shear modulus G is calculated using $G = \sqrt{G'^2 + G''^2}$ at $\omega = 1$ Hz.

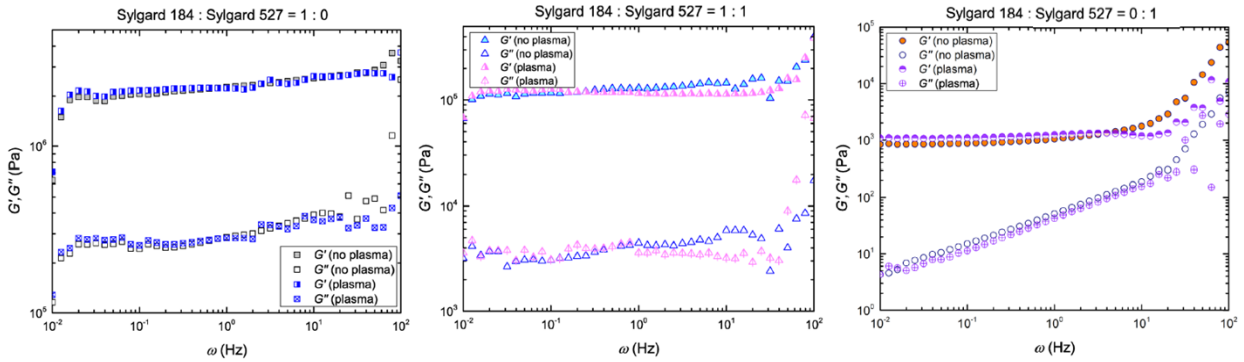

Figure S4. Rheology of soft substrates with plasma treatment. Variation of storage modulus (G') and loss modulus (G'') with angular frequency ω for substrates prepared combining Sylgard 184 PDMS (10:1) and Sylgard 527 (1:1) in different weight ratios for with and without plasma-treatment. The static shear modulus G is calculated using $G = \sqrt{G'^2 + G''^2}$ at $\omega = 1$ Hz.

(a)

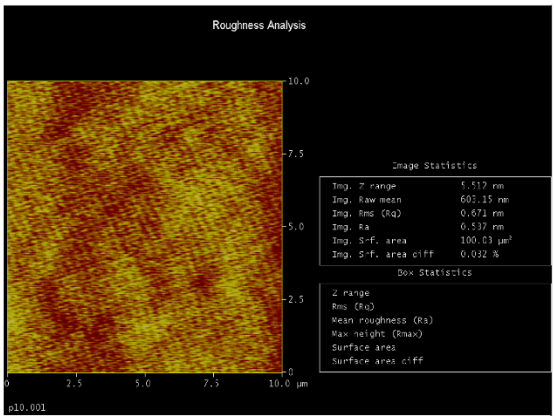

(b)

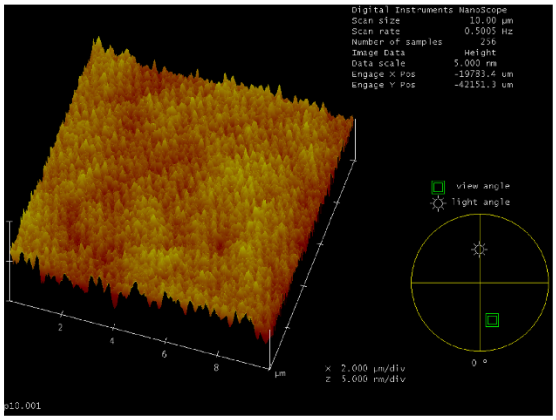

Figure S5. AFM measurements. (a) Atomic force microscopy (AFM) scan on a 10 µm × 10 µm cross-section of a plasma treated PDMS substrates with elastic modulus, $E_2 = 6855$ kPa. R_q and R_a values for the scan are shown. (b) Three-dimensional profile of the scan shown in (a).

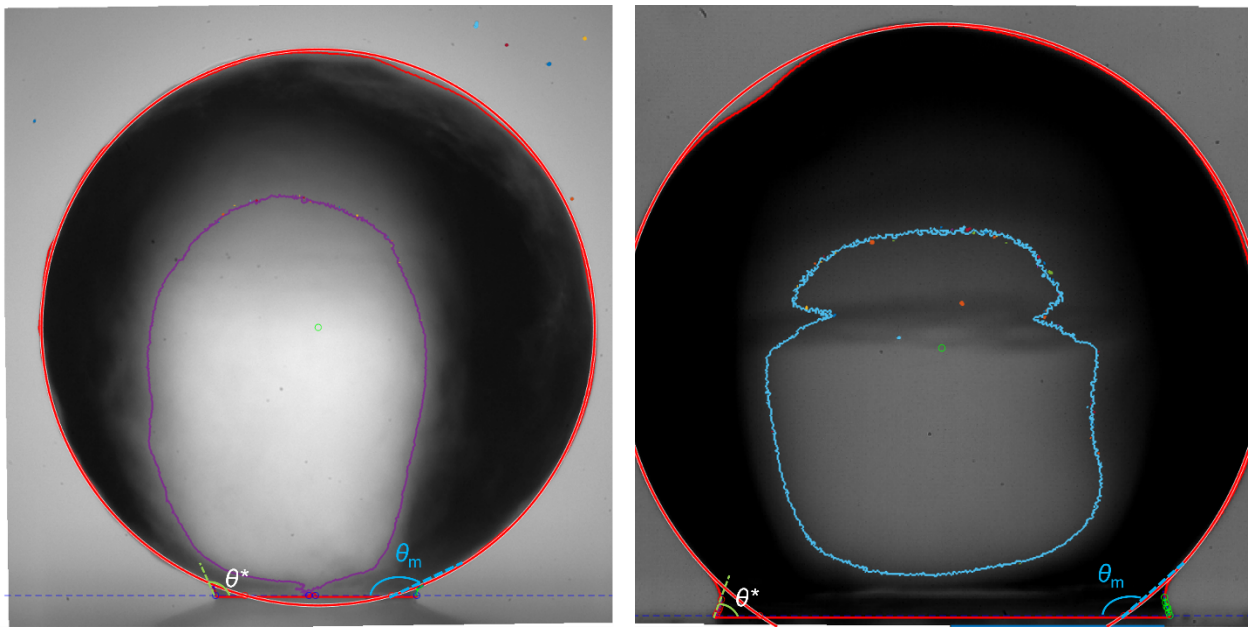

Figure S6. Experimental snapshots of hydrogels on surfaces highlighting the fitting procedure to extract the foot contact angle θ^* and apparent macroscopic angle away from the foot θ_m.

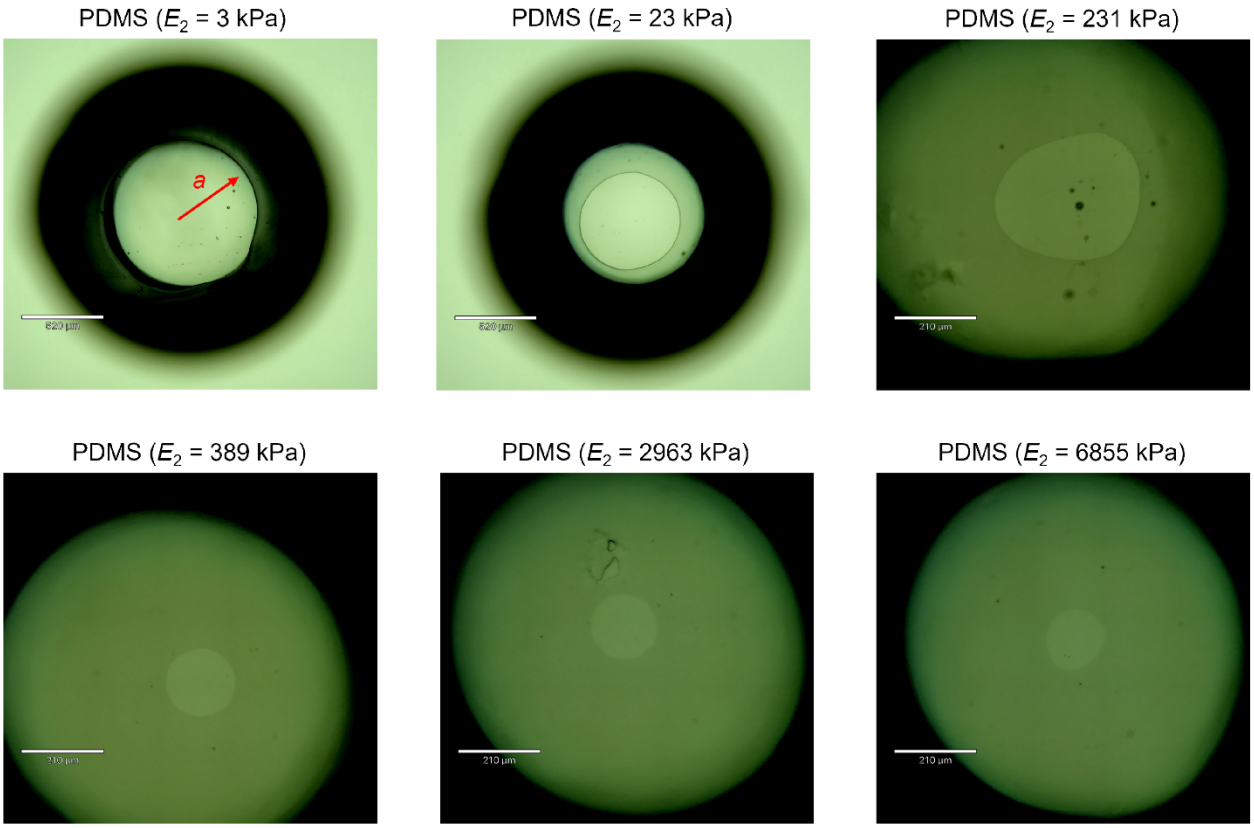

Figure S7. Glass sphere on soft PDMS. Bottom-view bright-field microscopy images of 1mm radius rigid glass spheres in contact with soft PDMS substrates for varying elasticity (E_2). a denotes the contact radius. Note the different scale bars.

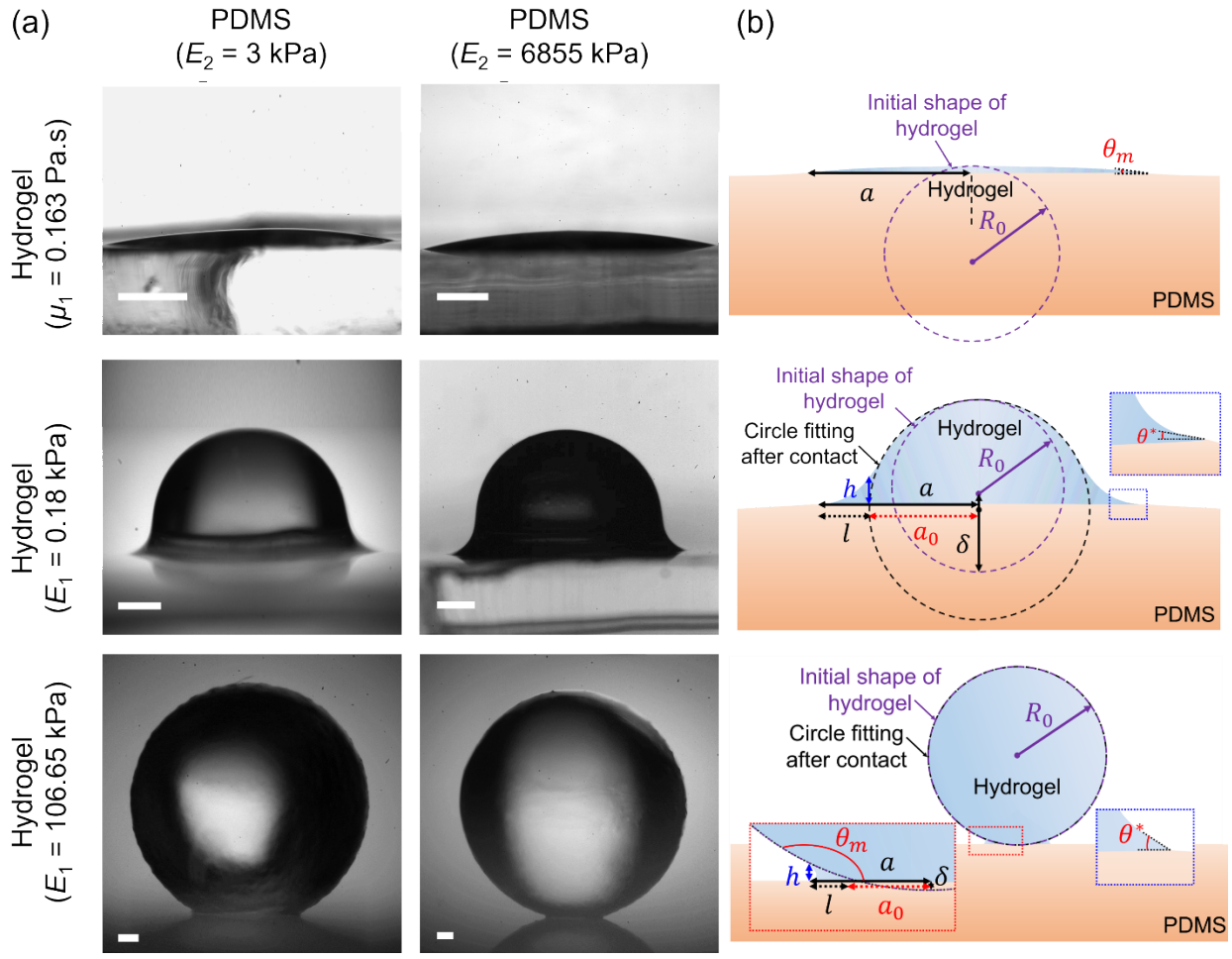

Figure S8. (a) Experimental snapshots of the static configuration of different hydrogels on plasma-treated soft substrates with elasticity $E_2 =$ 3 kPa and $E_2 =$ 6855 kPa. Scale bars represent 0.5 mm. (b) Schematics of the different possible hydrogel profiles of initial radius R_0 on the soft substrates. θ_m and θ^* are the macroscopic and foot contact angles, respectively. a and a_0 are the real and apparent contact radius, respectively. δ is the apparent indentation depth. h and l are the foot height and length, respectively.

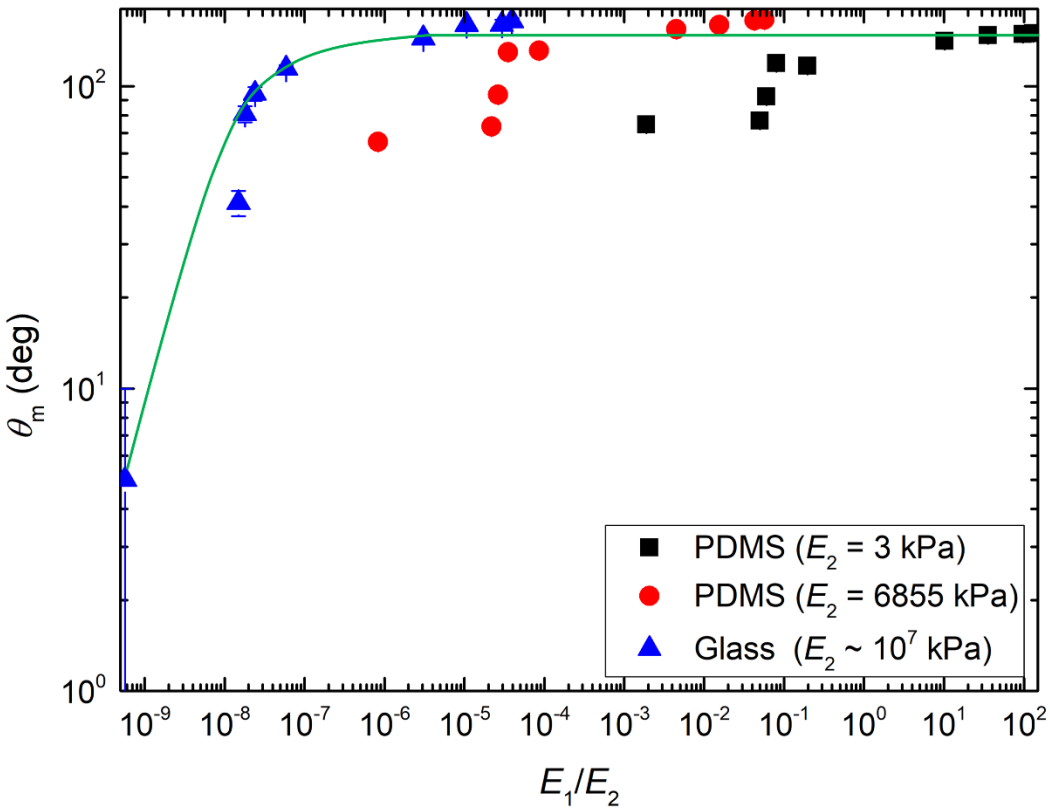

Figure S9: Variation of macroscopic contact angle θ_m with the elasticity ratio of the top (hydrogel, E_1) and bottom (PDMS, glass, E_2) pair E_1/E_2. The solid curve is a guide for the eye.

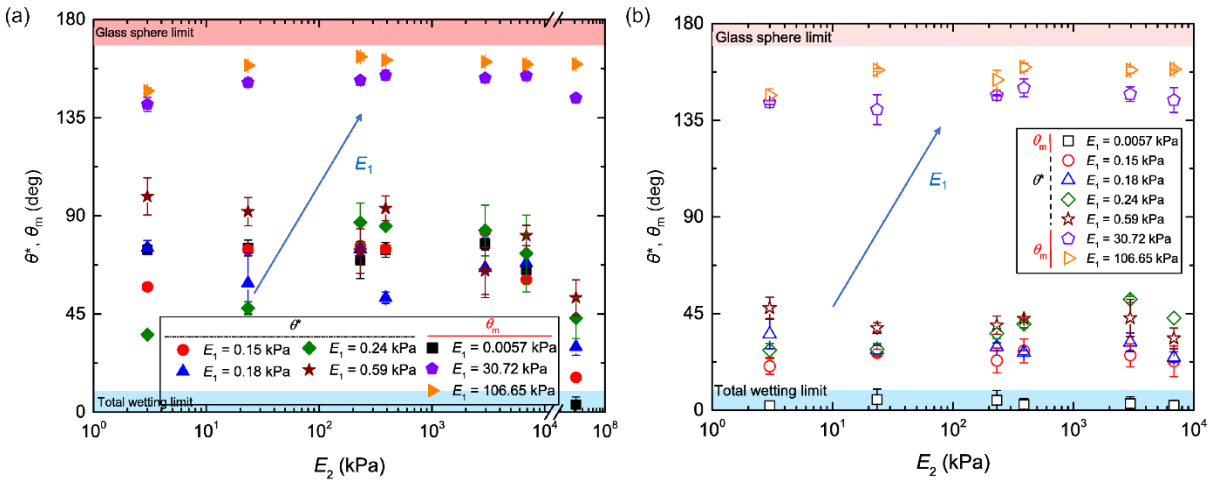

Figure S10. Hydrogel contact angles. Variation of contact angles (θ_m, θ^*) of hydrogels of varying elasticity (E_1) on pristine (a) and plasma treated (b), soft PDMS substrates of varying elasticity (E_2).

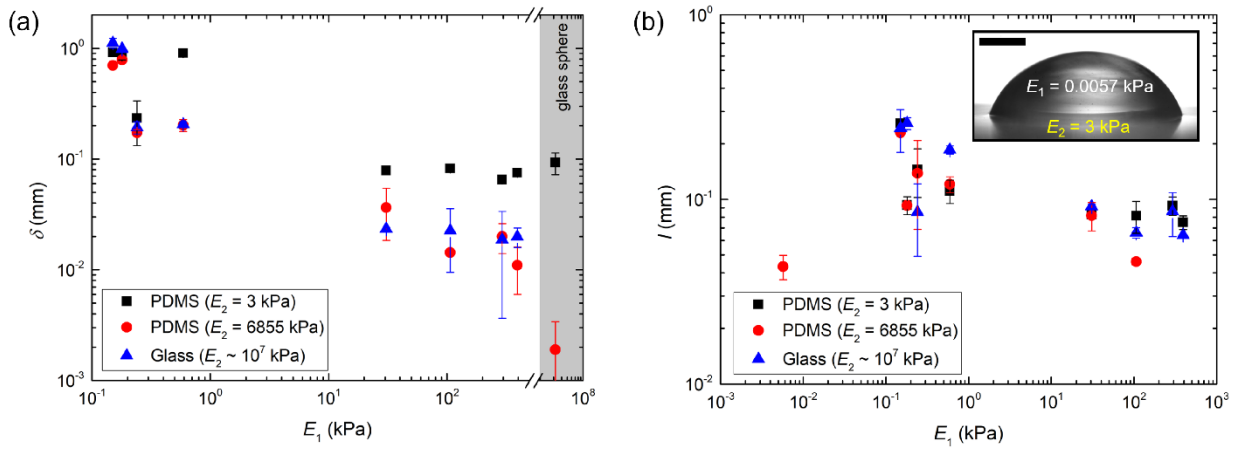

Figure S11. Variation of hydrogel contact radius (a), foot-height (b) for different hydrogel elasticity (E_1) on relatively soft PDMS ($E_2 = 3$ kPa), relatively stiff PDMS ($E_2 = 6855$ kPa) and rigid glass slides ($E_2 \approx 10^7$ kPa). The data for rigid glass sphere is also shown for (a). The hydrogel with the lowest elasticity, i.e., $E_1 = 0.0057\ kPa$ exhibits no foot on the softest PDMS substrate, i.e., $E_2 = 3$ kPa (inset of (b)). The radius of hydrogel is $R_0 \approx 1$ mm. All soft substrates are 2 mm thick.

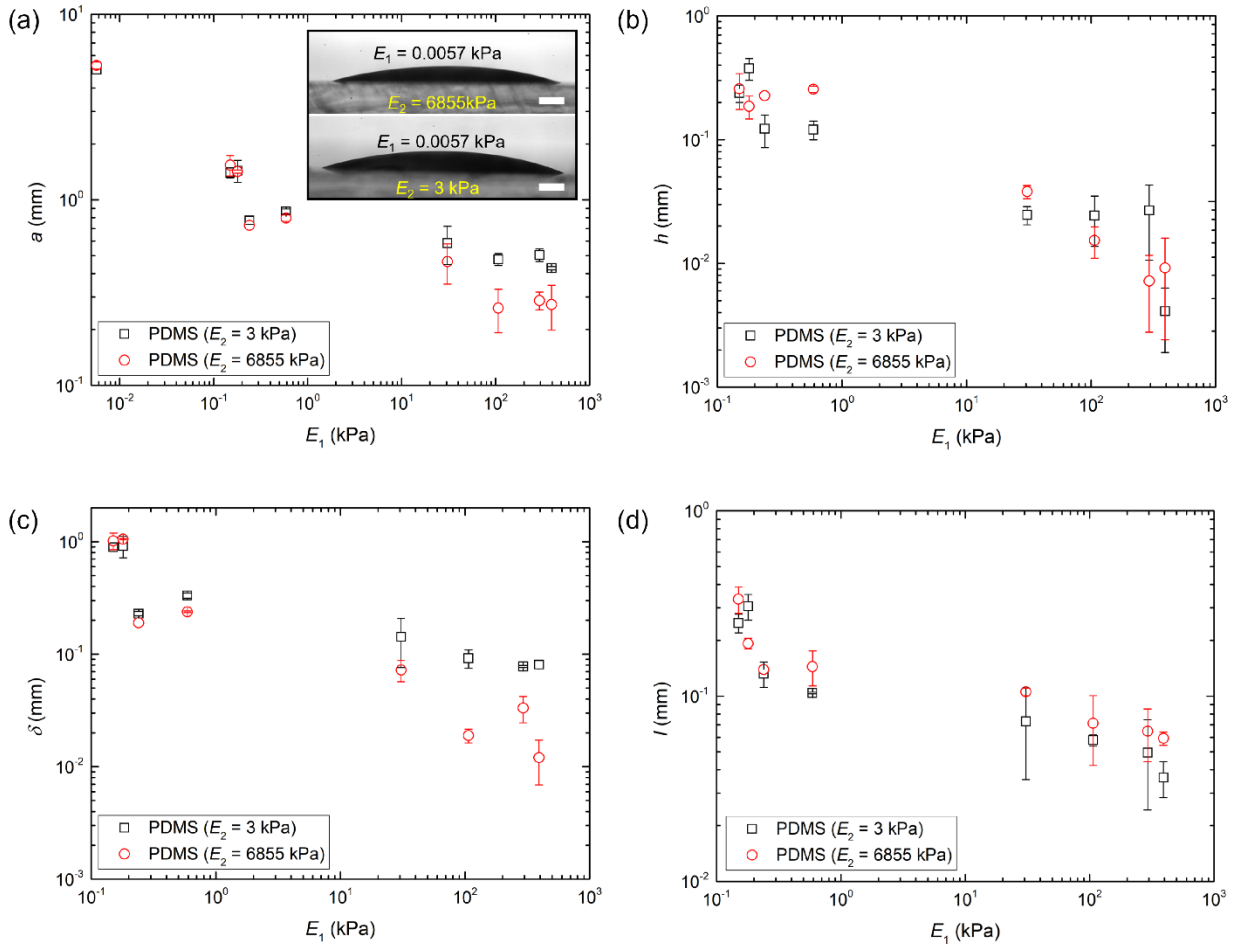

Figure S12. Hydrogels on plasma treated PDMS. Variation of hydrogel contact radius (a), foot- height (b), apparent indentation depth (c) and foot-length (d) for different hydrogel elasticity (E_1) on relatively soft PDMS ($E_2 =$ 3 kPa) and relatively stiff PDMS ($E_2 =$ 6855 kPa). The hydrogel with the lowest elasticity, i.e., $E_1 =$ 0.0057 kPa exhibits no foot on either of the plasma treated PDMS substrates (inset of (b)). The radius of hydrogel is $R_0 \approx$ 1 mm. All soft substrates are 2 mm thick.

S1.1 Adhesion measurements

For measuring the work of adhesion between hydrogel and PDMS, we used a cantilever-based force probe [1]. A polymeric capillary tube of diameter 410 μm and spring constant, $k = 305 \pm 6.1$ nN/μm is used as the cantilever probe. A hydrogel sphere/droplet was attached to the tip of the probe and the PDMS substrate (affixed to a linear actuator) was made to approach the probe at a prescribed velocity of 0.1 mm/s. Once contact was established, there was a hold time of 10-20 s after which the PDMS substrate was made to retract. The adhesion induced interaction between PDMS, and the hydrogel probe caused deflection x of the cantilever. Consequently, the maximum deflection Δx was measured, and the corresponding peak adhesion force was calculated using, $F = k\Delta x$ (Fig. S13). The work of adhesion is calculated using the relation for critical pull-off force: $F_{c,JKR} \approx 3\pi R_0 w/2$ [2,3] However, for the present case of different hydrogel contacts, we have added contributions to the above expression. The first added contribution comes from the capillary force from the hydrogel foot [4], $F_f \approx 2\pi R_0 \gamma\left(cos\theta^*_L + cos\theta^*_R\right) \approx 4\pi R_0 \gamma cos\theta^*$, where θ^*_L and θ^*_R are the foot contact angles. The second contribution comes from the capillary force from the spherical cap profile [5], $F_c \approx \pi\gamma(a^2 + b^2)/b$, where b is the vertical height of the hydrogel. Thus, the critical force becomes, $F \approx 4\pi R_0 \gamma cos\theta^* + \pi\gamma(a^2 + b^2)/b + 3\pi R_0 w/2.$ For example, for the experiment shown in Fig. S13, we obtain the peak (pull-off) force $F = 1.6$ mN. Consequently, using $\gamma = 61.9$ mN/m, $a \approx 0.48$ mm, $b \approx 1.97$ mm, $R_0 \approx 1$ mm, and $\theta^* \approx 50°$, we calculate $w \approx 128$ mN/m. Incidentally, the calculated adhesion force is close to that obtained using $w \approx 2\gamma$, an assumption extensively used in existing literature [4,6,7]. At the same time, the present observation indicates a few things. First, if the rationale of $w \sim (1+\cos\theta)\gamma$ is used for adhesion calculation, using θ_m would lead to reduced w for the stiffer hydrogels. Consequently, the data points in Fig. 7 of the main manuscript would shift to the right and fall beyond the JKR predictions. Thus, it is more likely that the microscopic foot contact angle θ* plays a role in dictating w. Since high accuracy in measuring θ* is currently not possible, the authors hypothesize that the foot curvature becomes highly acute in meeting the substrate and may achieve a value close to 0 which makes $w \sim 2\gamma$ appropriate for most of the hydrogels.

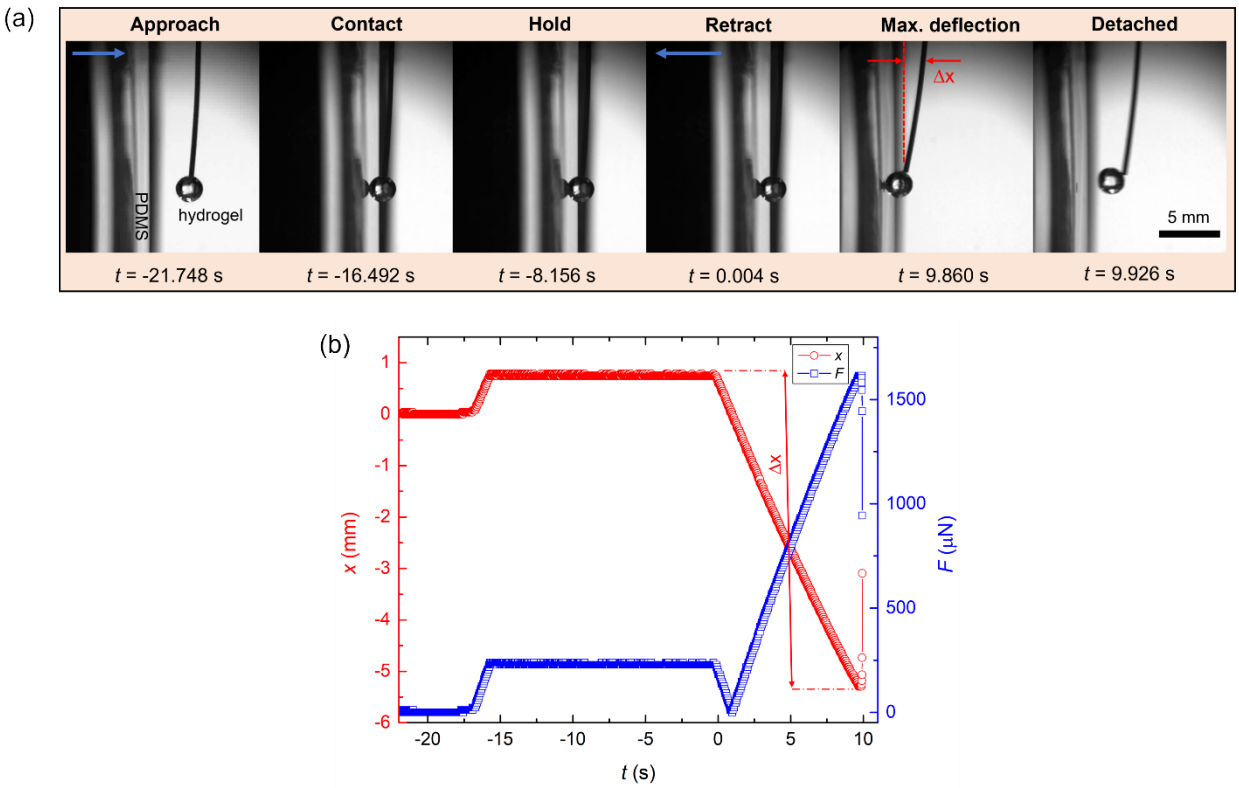

Figure S13. Cantilever-based force measurements. (a) Experimental snapshots of the cantilever-based contact force/adhesion measurements for a 1 mm radius hydrogel (E_1 = 106.65 kPa) with soft PDMS substrate (E_2 = 3 kPa). The different stages of force measurements: approach of the substrate, contact, hold, retraction of the substrate, maximum deflection of the cantilever and detachment are shown. $t \approx 0$ represents the onset of substrate retraction. Scale bars represent 5 mm. (b) Evolution of cantilever deflection x (measured) and force F (extracted) for the experiment shown in (a). Δx represents the maximum cantilever deflection. The blue arrows represent the direction of substrate motion.

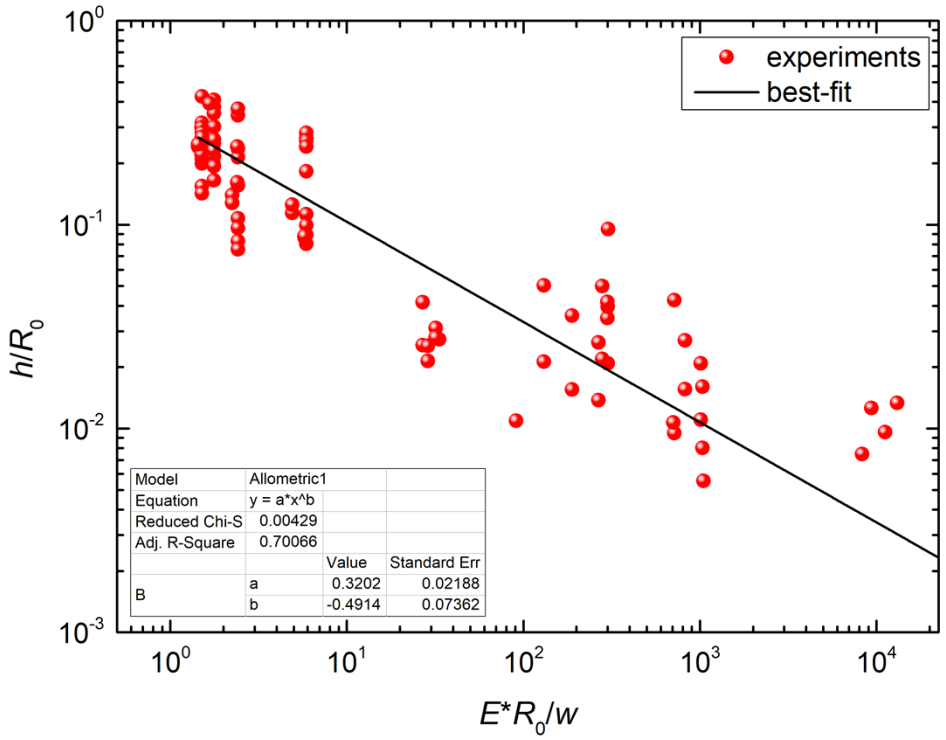

Figure S14: Variation of normalized foot height h/R_0 with the elasto-adhesive parameter E^*R_0/w for all the hydrogels on the different soft substrates shown in Fig. 8b of the main manuscript. The solid line represents the power-law best fit with an exponent of -0.49.

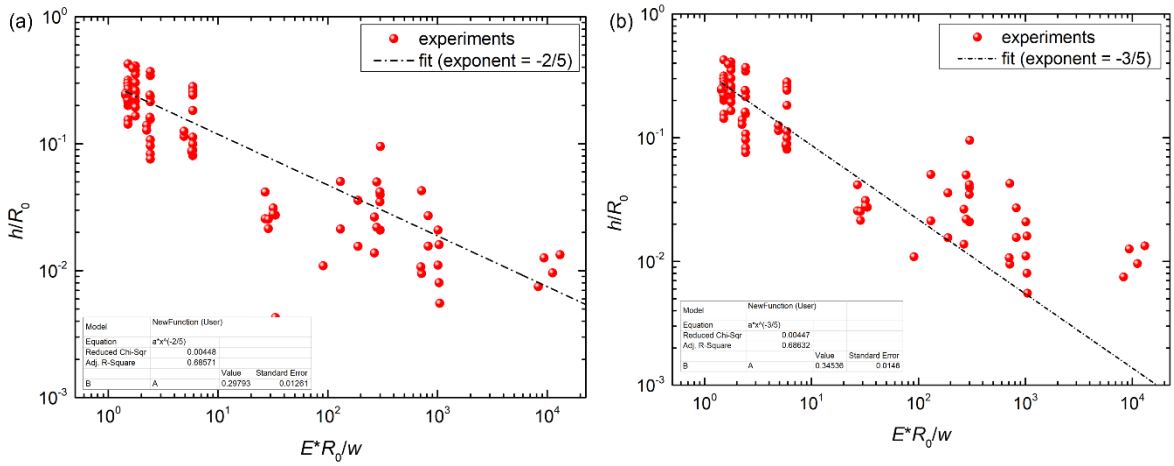

Figure S15: Variation of normalized foot height h/R_0 with the elasto-adhesive parameter E^*R_0/w for all the hydrogels on the different soft substrates shown in Fig. 8b of the main manuscript. The dotted lines represent the power-law fit with an exponent of (a) -0.4 and (b) -0.6.

S1.2 Detailed derivation of the relation between strain and elasto adhesive parameter (Eq.2 of the manuscript)

As highlighted in the main manuscript, for the small-to-large deformations present for the contact/wetting system of hydrogels on all the surfaces used , the appropriate elastic energy U_{el} can be expressed as [5,8,9]:

$$U_{el} \sim E^* R_0^3 \int_0^{a/R_0} \left[\frac{1}{2} - \frac{(1+x'^2)}{4x'} ln\left(\frac{1+x'}{1-x'}\right)\right]^2 dx' \quad \text{(S1)}$$

where, $E^* = [(1-\nu_1^2)/E_1 + (1-\nu_2^2)/E_2]^{-1}$. Here, E_1, ν_1 and E_2, ν_2, elastic moduli and Poisson's ratios of the top (hydrogel) and bottom (glass, PDMS) pair, respectively. R_0 is the hydrogel radius, a is the contact radius, and $x' = a/R_0$ is the normalized contact radius or strain. Consequently, using the approximation, $\ln[(1+x')/(1-x')] \approx 2\tanh^{-1} x'$ we can express the elastic energy as,

$$U_{el} \approx E^* R_0^3 \int_0^{a/R0} \left[\frac{1}{2} - \frac{(1+x'^2)}{4x'} 2\tan^{-1} x\right]^2 dx' \quad \text{(S2)}$$

Consequently, using the approximation, $2\tanh^{-1} x' \approx 2\left(x' + \frac{x'^3}{3}\right)$, we can express U_{el} as,

$$U_{el} \approx E^* R_0^3 \int_0^{a/R_0} \left[\frac{1}{2} - \frac{(1+x'^2)}{2x'}\left(x' + \frac{x'^3}{3}\right)\right]^2 dx' \quad \text{(S3)}$$

Upon evaluating all the algebraic terms within the third bracket, we arrive at

$$U_{el} \approx E^* R_0^3 \int_0^{a/R0} \frac{1}{4}\left[-\frac{x'^4}{3} - \frac{4x'^2}{3}\right]^2 dx' \quad \text{(S4)}$$

Upon evaluating the squared term, we arrive at the final form of the integral,

$$U_{el} \approx E^* R_0^3 \int_0^{a/R0} \frac{1}{36}(x'^8 + 8x'^6 + 16x'^4) dx' \quad \text{(S5)}$$

Consequently, evaluating the integral within the limit 0 and a/R_0, we obtain the final algebraic form of the elastic energy U_{el},

$$U_{el} \approx \frac{E^* R_0^3}{36}\left[\frac{1}{9}\left(\frac{a}{R_0}\right)^9 + \frac{8}{7}\left(\frac{a}{R_0}\right)^7 + \frac{16}{5}\left(\frac{a}{R_0}\right)^5\right] \quad \text{(S6)}$$

Therefore, the total energy can be expressed as, $U = U_{el} + U_{ad} = U_{el} - \pi w a^2$. Upon minimizing with respect to the contact radius a, i.e., $\frac{\partial U}{\partial a} = 0$, we obtain

$$\frac{E^* R_0^2}{36}\left[\left(\frac{a}{R_0}\right)^8 + 8\left(\frac{a}{R_0}\right)^6 + 16\left(\frac{a}{R_0}\right)^4\right] - 2\pi w a = 0 \quad \text{(S7)}$$

Upon rearranging the terms, we obtain the final algebraic relation between strain a/R_0 and the elasto- adhesive parameter $E^* R_0/w$:

$$\left[\left(\frac{a}{R_0}\right)^7 + 8\left(\frac{a}{R_0}\right)^5 + 16\left(\frac{a}{R_0}\right)^3\right] = \frac{72\pi w}{E^* R_0} \quad \text{(S8)}$$

Thus, we obtain Equation 2 in the main manuscript.

References:

[1] S. Shyam, S. Misra, S. K. Mitra, J. Colloid Interface Sci. 2023, 630 322.

[2] K. L. Johnson, K. Kendall, A. D. Roberts, Proc. Royal Soc. Lon. A. 1971, 324, 1558 301.

[3] P. Prokopovich, V. Starov, Adv. Colloid Interface Sci. 2011, 168, 1-2 210.

[4] H.-J. Butt, B. Cappella, M. Kappl, Surf. Sci. Rep. 2005, 59, 1-6 1.

[5] T. Salez, M. Benzaquen, E. Raphael, Soft Matter 2013, 9, 45 10699.

[6] K.-K. Liu, J. Phys. D: Appl. Phys. 2006, 39, 11 R189.

[7] A.-R. Kim, S. K. Mitra, B. Zhao, J. Colloid Interface Sci. 2022, 628 788.

[8] D. Maugis, *Langmuir*, 1995, 11, 679–682.

[9] D. Maugis, D., M. Barquins, *J. Phys. D: Appl. Phys.*,1983, *16*(10), 1843.